

Rutherford Scattering

Nestor Viana
Florida International University

December 2nd, 2019

1 Introduction

In 1909, Hans Geiger and Ernest Marsden carried out experiments to study the scattering of alpha particles by thin metal foils under the supervision of Ernest Rutherford in his laboratory. Surprisingly, they observed back-scattering at angles greater than 90 degrees, which seemed impossible according to J.J. Thompson's plum-pudding model of the atom (Figure 1). If positive charge were evenly distributed throughout the mass of the atoms, α -particles at most should have scattered at small angles due to weak Coulomb interactions. Rutherford theorized that such event was possible only if positive charge were instead tightly packed in a region within the atom, contradicting Thompson's model. He discovered a mathematical expression that predicted the nature of scattering based on differential cross-sections,

$$\frac{d\sigma}{d\Omega} = \left(\frac{zZe^2}{16\pi\varepsilon_0 E} \right)^2 \frac{1}{\sin^4(\theta/2)} \quad (1)$$

where z and Z are the charges of the α -particle and the nucleus of the target, ε_0 is the vacuum permittivity, E is the kinetic energy of the α -particles, and θ is the scattering angle.

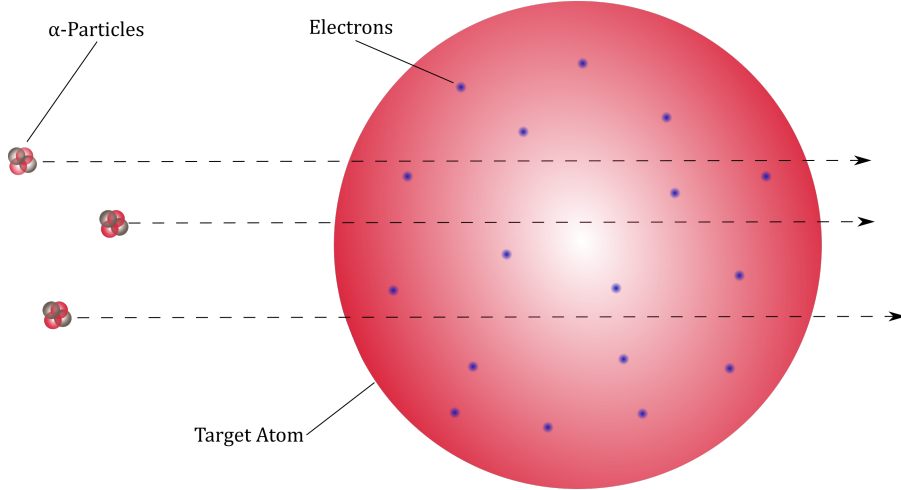


Figure 1: J.J. Thompson's atomic model interaction with α -particles.

The differential cross-section $d\sigma/d\Omega$ for scattering from a single particle is defined as¹

$$\frac{d\sigma(\theta, \varphi)}{d\Omega} = \frac{\text{flux scattered into element } d\Omega \text{ at angles } \theta, \varphi}{\text{Incident flux per unit area}} \quad (2)$$

Therefore the cross-section σ has units of area and could be interpreted as the area of the scattering center projected on the plane normal to the incoming beam. The differential solid angle $d\Omega$ is described in Figure 2 below. Note that

$$\int_0^{2\pi} \int_0^\pi \frac{d\sigma}{d\Omega} \sin \theta d\theta d\varphi = \sigma$$

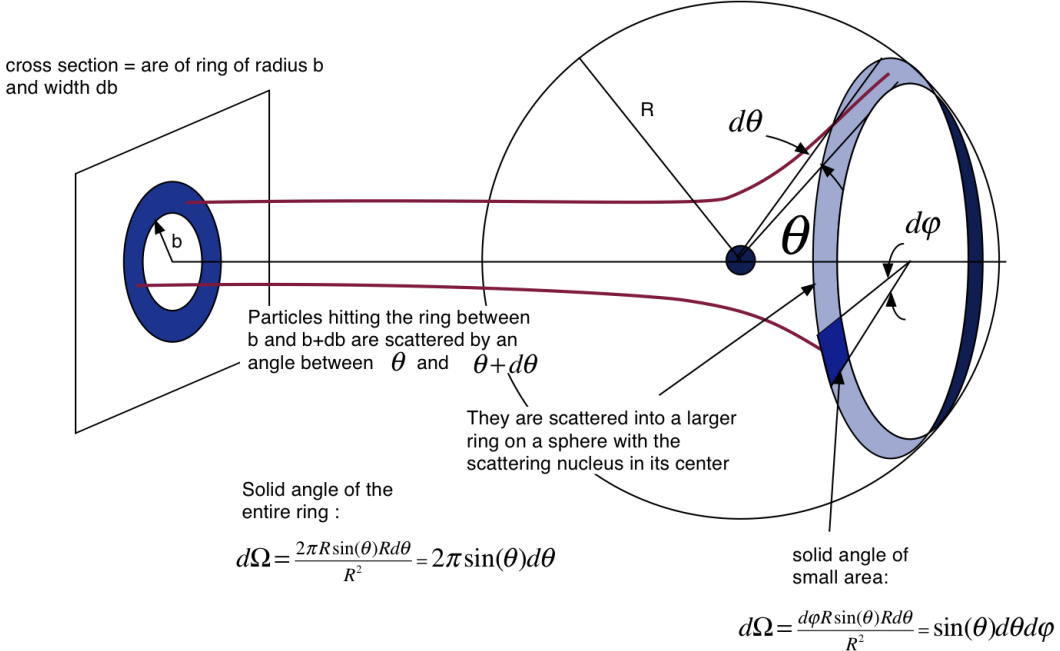


Figure 2: Geometry of the cross section and the solid angle.

In this experiment, we want to calculate the rate of particles scattered \dot{N} at an arbitrary angle θ which can be obtained by

$$\dot{N} = \left(\begin{array}{c} \text{Rate of incident} \\ \alpha\text{-particles} \end{array} \right) \times \left(\begin{array}{c} \# \text{ of target nuclei} \\ \text{per unit area} \end{array} \right) \times \left(\begin{array}{c} \text{Solid angle} \\ \text{of detector, } d\Omega \end{array} \right) \times \left(\begin{array}{c} \text{Single-particle} \\ \text{cross-section} \end{array} \right)$$

The rate of incident α -particles, \dot{N}_i is computed using the source strength S_α , the target area A_T , and the distance between the source and the target D by

$$\dot{N}_i = \frac{S_\alpha A_T}{4\pi D^2}. \quad (3)$$

A small piece of gold foil of thickness t , density ρ , and area A has mass

$$M_A = \rho A t$$

The number of nuclei n contained in the small piece is

$$n = \frac{M_A}{\mathcal{M}} N_a = \frac{\rho A t N_a}{\mathcal{M}},$$

where \mathcal{M} is the molar mass of gold. Therefore the number of target nuclei per unit area is

$$\frac{n}{A} = \frac{\rho t N_a}{\mathcal{M}} \quad (4)$$

For detectors with small openings, the solid angle is defined as

$$d\Omega = \frac{A_{det}}{R^2} \quad (5)$$

where A_{det} and R are the effective detector area and the distance between the detector and the target foil, respectively. Substituting Equations 1, 3, 4, and 5 into the scattering rate expression gives

$$\dot{N} = \frac{S_\alpha A_T}{4\pi D^2} \frac{\rho t N_a}{\mathcal{M}} \frac{A_{det}}{R^2} \left(\frac{z Z e^2}{16\pi \epsilon_0 E} \right)^2 \frac{1}{\sin^4(\theta/2)} \quad (6)$$

2 Experimental Setup

We utilize a vacuum chamber with a rotatable Americium-241 source, a foil target mount, and a semiconductor detector. The detector is connected to a pre-amplifier, then to an amplifier together with a multi-channel analyzer (MCA) (Figure 3).

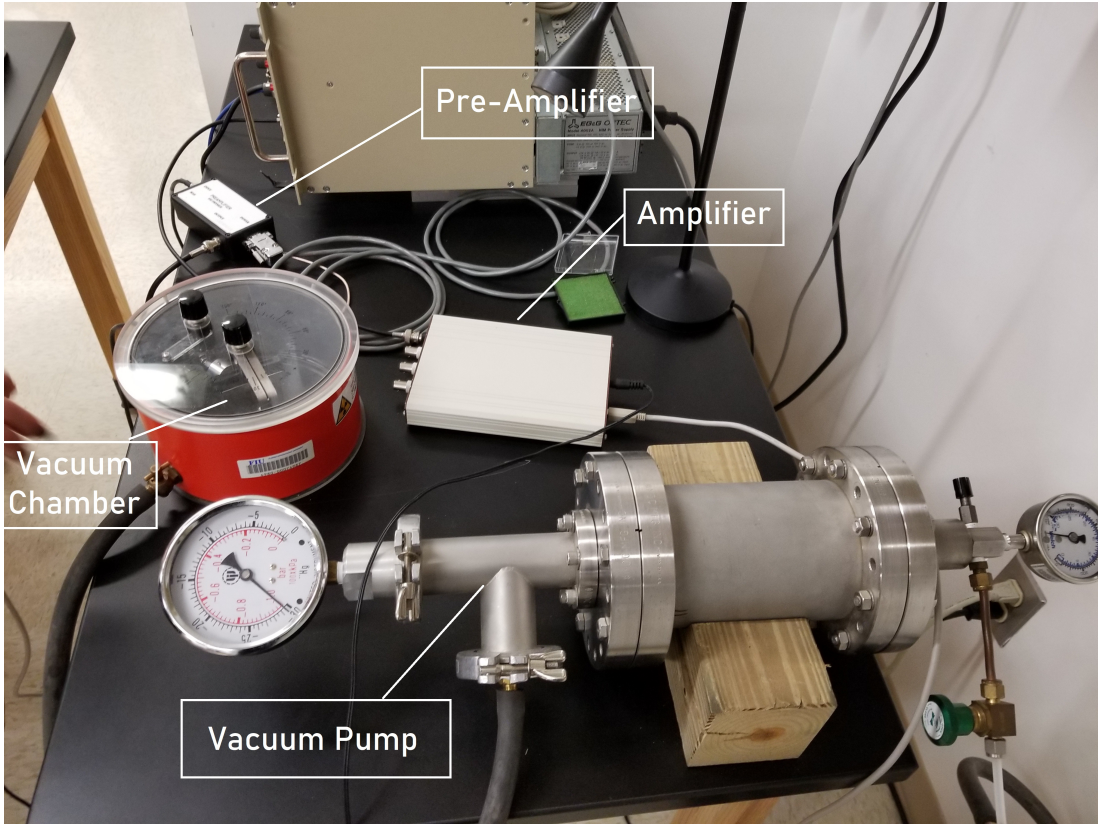


Figure 3: Equipment setup.

We fix the ^{241}Am source and place the gold foil holder onto the target mount. The thickness t of the gold foil is $2 \mu\text{m}$. Before starting the vacuum pump, we close the chamber, rotate the source at a 0° angle, close the valve, and connect the hose to the pump. Then we turn the pump on and open the valve slowly to let air exit the chamber for about 20 seconds.

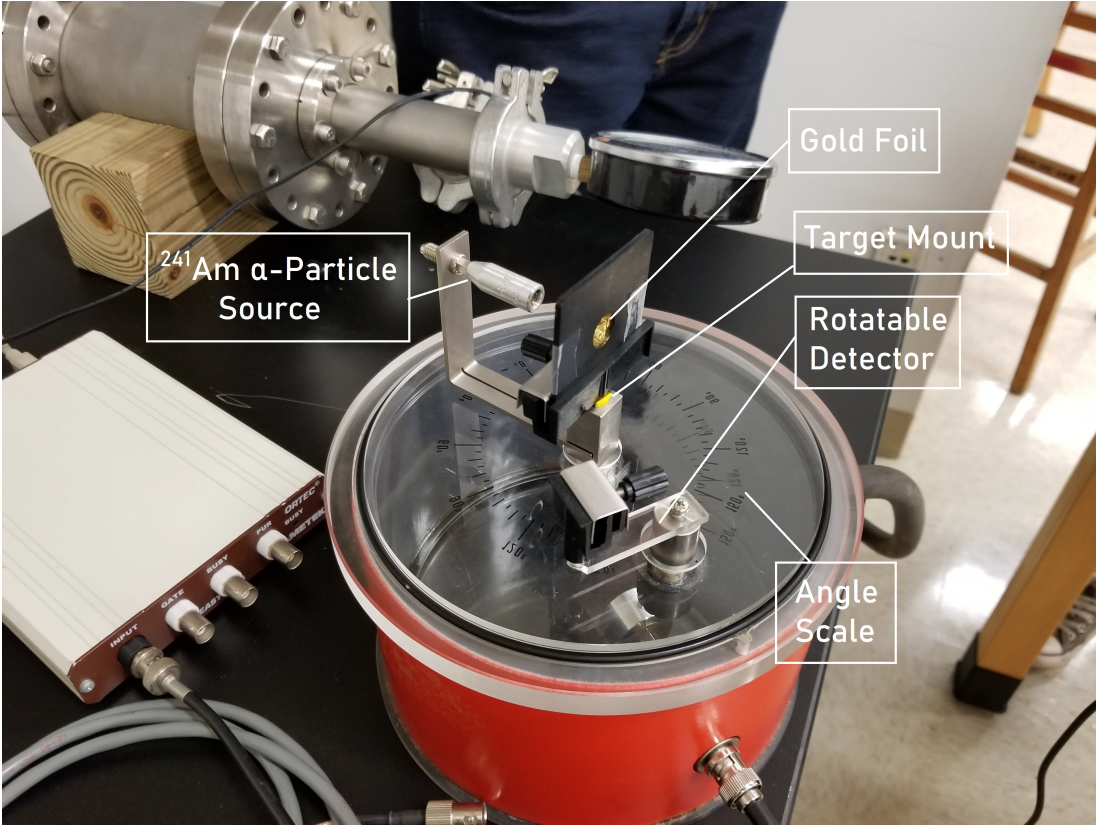


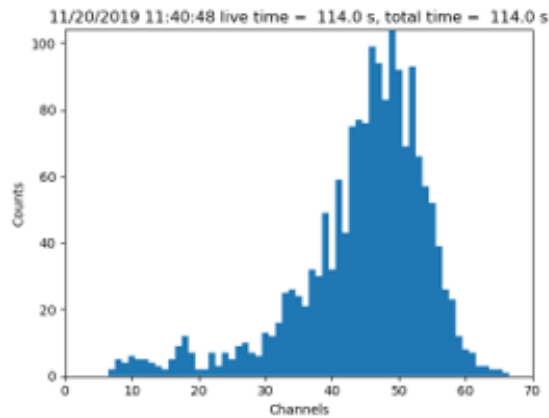
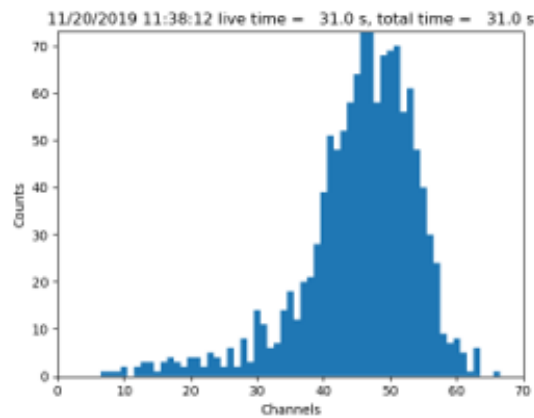
Figure 4: Setup inside the vacuum chamber.

To start taking data, we set the multi-channel analyzer live time to 300 seconds and let the count spectrum develop until it shows around 1000 counts around the peak. This will correspond to an error of about 3% in the data. We repeat these steps at angles $\pm 5^\circ$, $\pm 10^\circ$, $\pm 15^\circ$, $\pm 20^\circ$, and -25° while adjusting the live time appropriately to obtain counts with errors 3% for $\pm 5^\circ$, 5% for $\pm 10^\circ$, 7% for $\pm 15^\circ$, and 10% for the rest.

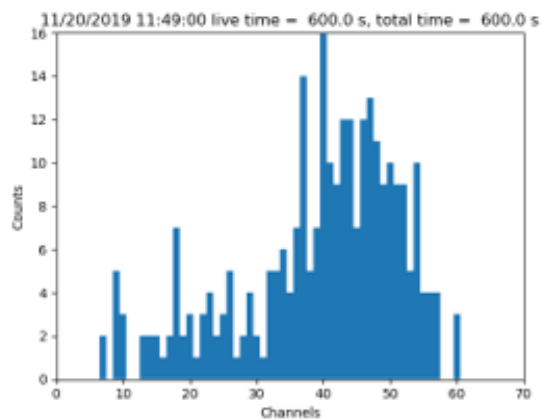
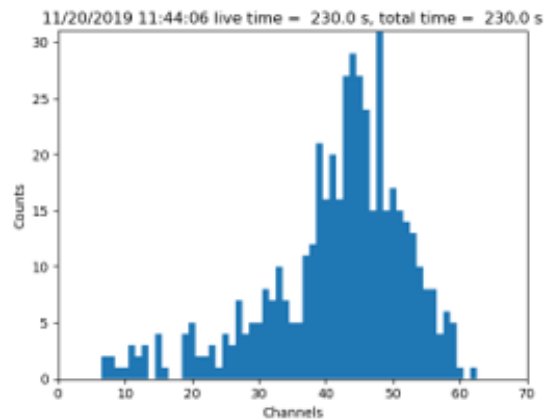
3 Data

In the next page we show the plots of the count spectra for all the angles in the procedure described previously. According to Equation 6, we expect very high count rates for the small angles and very low rates as the scattering angle θ increases, thus lengthening the time required for the graphs to develop. We stop taking data once we reach the desired error in the counts. For positive angles (counterclockwise rotations of the source), notice that the peaks mostly develop around the 35-60 channel ranges, whereas the peaks shift to 45-75 ranges for negative angles (clockwise rotation).

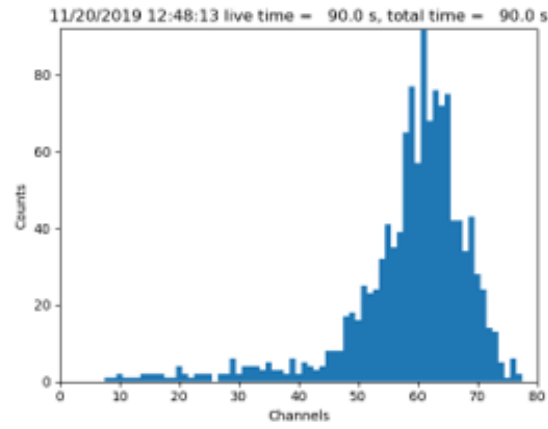
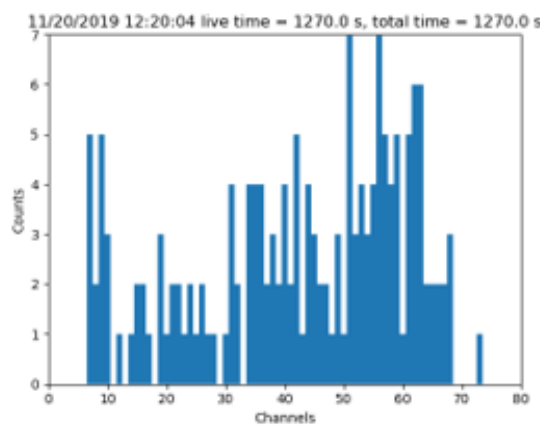
However, we would expect the channel ranges for negative and positive angles to be the same, therefore the most be an angle offset θ_0 as we started rotating the ^{241}Am source in the negative direction. We will analyze this factor in more detail in the analysis section.



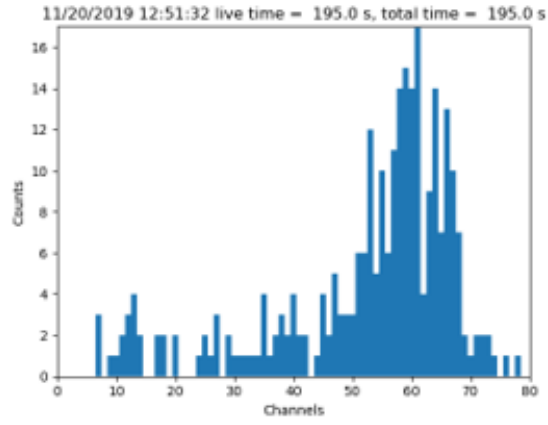
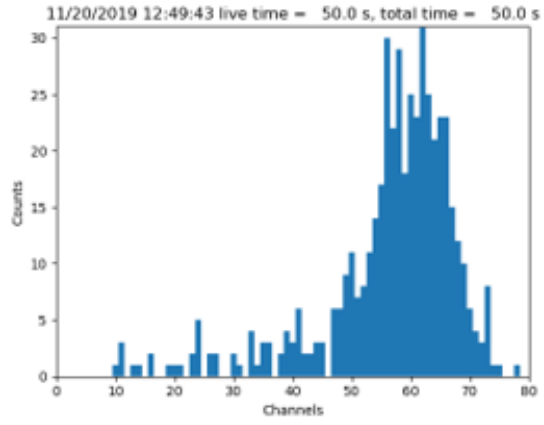
Count spectra for 0° and 5°.



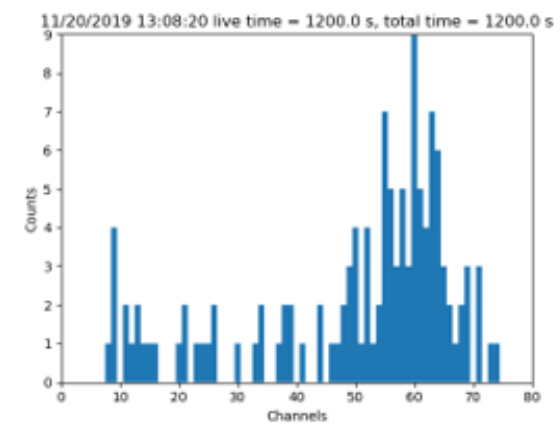
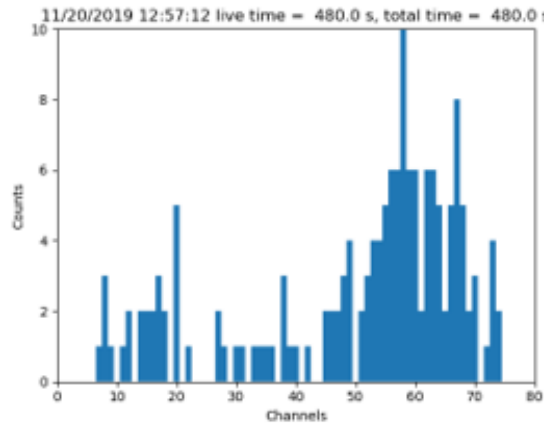
Count spectra for 10° and 15°.



Count spectra for 20° and -5°.



Count spectra for -10° and -15° .



Count spectra for -20° and -25° .

4 Analysis & Results

Studying the graphs above lets us determine the count rates $\dot{N} = N/t$, where N is the number of counts within each peak and t is the live time, for each scattering angle θ which be tabulate below.

θ (degrees)	Counts N	Live Time t (seconds)	Count Rate \dot{N} (counts/sec)
0	1105	31	35.645
5	1435	114	12.587
10	375	230	1.630
15	206	600	0.343
20	86	1270	0.067
-5	965	90	10.722
-10	363	50	7.260
-15	177	195	0.907
-20	94	480	0.195
-25	72	1200	0.060

To examine the validity of the scattering rate expression, we plot a graph of $\log(\dot{N})$ vs $\log(\sin \theta/2)$. We should expect a linear relationship between these quantities if the rate expression is correct. Taking the logarithm of both sides of the expression for \dot{N} and differentiating gives us the error for this graph as

$$\sigma_{\log \dot{N}} = \frac{\log e}{\sqrt{N}} \quad (7)$$

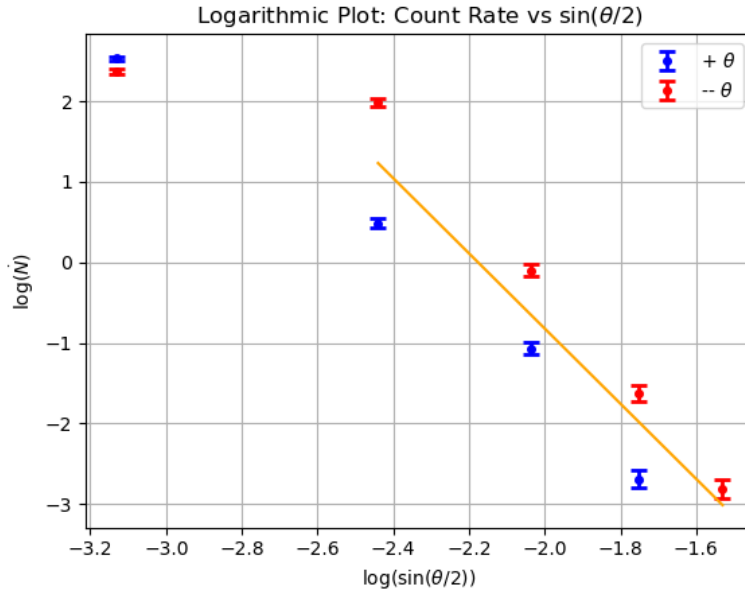


Figure 5: Logarithmic plot of the count rate \dot{N} against $\sin \theta/2$. The blue and red data points indicate counts taken at a clockwise and counterclockwise rotation of the α -particle source, respectively. We left out the data for $\theta = 0^\circ$ as this would make the graph diverge.

Evidently, Figure 5 shows a linear relationship between \dot{N} and $1/\sin^4(\theta/2)$ for angles $|\theta| \geq 10^\circ$. If we were to fit lines among the blue and red data points only, the slope would have roughly the same

value of (-3.827 ± 0.477) , confirming that the rate count decreases exponentially with respect to the scattering angle.

The error in the total number of counts at any scattering angle is given by

$$\sigma_N = \sqrt{N}. \quad (8)$$

Thus the error in the count rate is

$$\sigma_{\dot{N}} = \frac{\sqrt{N}}{t}. \quad (9)$$

To estimate the offset θ_0 , let us write Equation 6 as

$$\dot{N} = \frac{C_0}{\sin^4\left(\frac{\theta-\theta_0}{2}\right)} \quad (10)$$

and plot a nonlinear fit of this function with parameters C_0 and θ_0 in Figure 6.

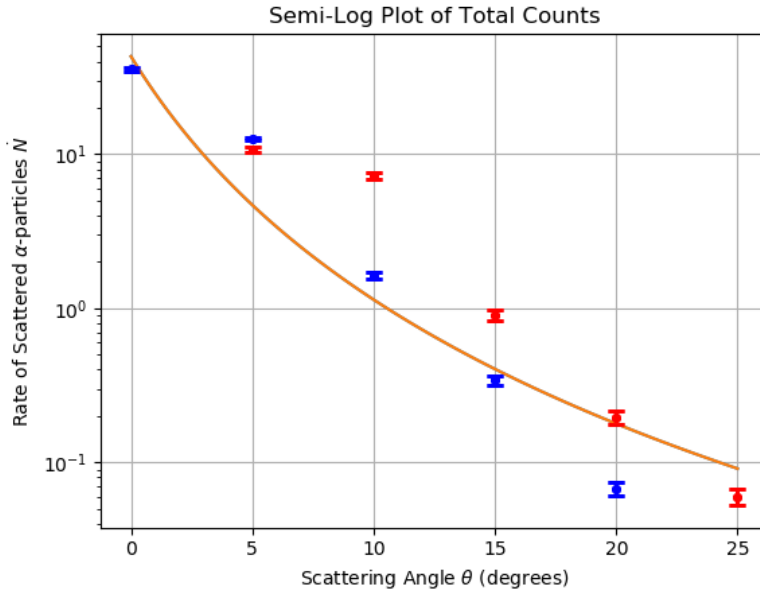


Figure 6: Semi-log plot of nonlinear fit of the count rate against the scattering angle.

The regression returns the values

$$C_0 = (50.89 \pm 1.93) \times 10^{-5} \text{ (counts/s)} \quad \text{and} \quad \theta_0 = 6.166^\circ \pm 0.001^\circ$$

5 Conclusion

As evidenced by the count spectra for $\theta = 20^\circ, -20^\circ$, and -25° , the counts were relatively much shorter than at the smaller angles and were much more spread out over the channels, leading to more variation in the total number of counts. Although this may not be as obvious since both Figure 5 and 6 do not show the size of the error bars appreciably, we can see that the count rates of these angles present the highest errors in our data. In fact, if we utilize Equation 7 to carefully explore the uncertainties, we obtain

θ (degrees)	$\sigma_{\log \dot{N}}$
0	0.03008
5	0.02640
10	0.05164
15	0.06967
20	0.10783
-5	0.03219
-10	0.05249
-15	0.07516
-20	0.10314
-25	0.11785

which agrees with the variation we just discussed. Our result for the angle offset $\theta_0 = 6.166^\circ \pm 0.001^\circ$ explains the shift of the peak centers of the count spectra from about 49 to 60 channels between the positive and negative scattering angles. This is surprisingly a big offset which may be due to the non-uniform texture of the gold foil surface whose effect factored in as we rotated the ^{241}Am source in the clockwise direction. Going back to Figure 5, we indeed did observe a linear relationship between the count rate \dot{N} and $1/\sin^4(\theta/2)$ for angles $|\theta| \geq 10^\circ$. Such relationship deviates at small θ because of the nature of the logarithmic function as it tends to diverge for arguments approaching the value of zero. The linear regression returned a value of $m = -3.827 \pm 0.477$ for the slope which merely confirms a strong exponential decrease relation between the scattering angle and the count rate, adding up to Rutherford's differential cross-section formula and overall to his hypothesis of a nucleus of positive charge within the atom.

6 References

- [1] "Interactions of Charged Particles with Photons and Matter." Experiments in Modern Physics, by Adrian C. Melissinos and Jim Napolitano, Academic Press, 2003, pp. 298–300.